Few-cycle spatiotemporal soliton wave excited by filamentation of a femtosecond laser pulse in materials with anomalous dispersion

Jiansheng Liu,* Ruxin Li, and Zhizhan Xu
State Key Laboratory of High Field Laser Physics, Shanghai Institute of Optics and Fine Mechanics, Chinese Academy of Sciences, P. O. Box 800-211, Shanghai 201800, People's Republic of China
(Received 15 May 2006; published 2 October 2006)

The nonlinear dynamics of 1.6-μm fs laser pulses propagating in fused silica is investigated by employing a full-order dispersion model. Different from the x-wave generation in normally dispersive media, a few-cycle spatiotemporally compressed soliton wave is generated with the contrary contributions of anomalous group velocity dispersion (GVD) and self-phase-modulation. However, at the tailing edge of the pulse forms a shock wave which generates separate and strong supercontinuum peaked at 670 nm. It is also the origin of conical emission formed both in time and frequency domain with the contribution of normal GVD at visible light.

DOI: 10.1103/PhysRevA.74.043801 PACS number(s): 42.65.Sf, 42.65.Tg, 42.65.Jx

The nonlinear propagation of a femtosecond laser pulse through transparent optical media has been widely studied both theoretically and experimentally for many years and still attracted considerable attentions since a large variety of unique phenomena and applications can be found such as white light production [1–3], pulse compression [4–7], remote sensing using lidar [8]. Since the first observation of self-trapping of optical beams at the very dawn of nonlinear optics [9], quite a number of models have been developed to explain the nonlinear processes of laser pulses propagating in optical media [10–19]. It is now well recognized that self-phase-modulation (SPM), dispersion, diffraction, and plasma behavior are the main causes of what we have observed such as supercontinuum generation, pulse splitting, *X* waves in the nonlinear propagation of such laser beam. These processes usually originate from the early self-focusing of the laser beam, leading to an explosive increase in the peak intensity if the input power is sufficiently high. The catastrophic collapse of the beam can be arrested by either dispersion or plasma generation [16–19], where the peak laser intensity is clamped. The resulting laser beam can self-channel to a long distance of many Rayleigh lengths and is generally accompanied by supercontinuum (SC) generation and colored conical emission which has been explained in different ways such as Čerenkov process, four-photon parametric process, and plasma process [20–22]. Recently, Kolesik *et al.* proposed dynamic nonlinear *X* waves for femtosecond pulse propagation in water and make use of the three-wave mixing picture to qualitatively explain the cause of *X* waves [17].

For the moment, most attention was paid on femtosecond laser pulses propagating in optical media with normal group velocity dispersion (GVD) which plays a very important role in the formation of dynamic *X* wave and pulse splitting in solid or liquid media [16–18]. Recent work indicates that a space-frequency coupling mainly from the interplay among SPM, normal GVD, and phase mismatching will reshape the laser beam into a conical wave and form a dynamic *X* wave [18]. The formation and role of conical emission as well as self-compression have also been analyzed there. Hauri *et al.* have also demonstrated the generation of few-cycle pulses via filamentation of 800 nm fs laser pulse in noble gases [6,23]. However, fewer studies were devoted to the physics of filamentation of fs laser pulses in media with anomalous dispersion [24,25], i.e., the nonlinear dynamics of infrared (at 1.5 μm or longer) femtosecond laser pulses propagating in silica or BK7 glass. Experimental results indicate that anomalous GVD favors a longer self-guiding of the laser beam compared to normal GVD [24]. Recent experimental work on the propagation of fs laser pulse at 1.5 μm in silica glass indicates that separate and strong SC peaked at 650 nm is generated [26]. It is quite different from SC generated from filamentation of 800 nm fs laser pulse and has not yet theoretical prediction. Since SC covers a quite large range from 400 to 3000 nm which supports the generation of few cycle pulses, one promising application is that using SPM to broaden the spectra and then compressing the laser pulse, it is possible to obtain an infrared few-cycle laser pulse which has advantages in producing much higher-order harmonic emissions since the cutoff frequency is defined as $E_{\max}=I_p$

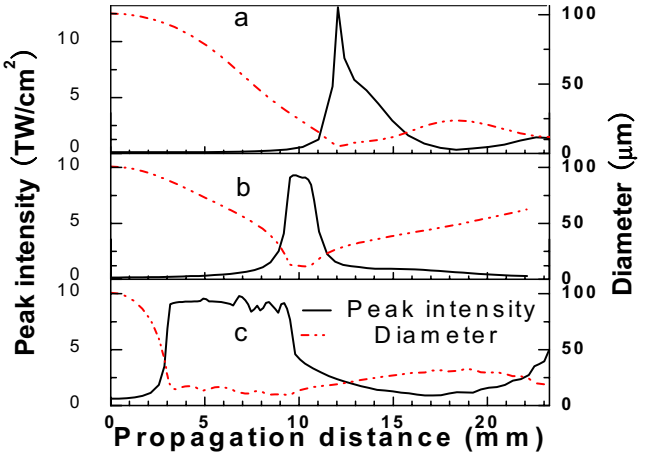

FIG. 1. (Color online) Evolution of peak intensities (solid curves) and beam diameters (FWHM, dashed curves), respectively, for different laser pulses with durations of 50 fs and radii of 87 μm. The central wavelengths and powers of the input pulses are (a) $\lambda=800$ nm, $P=14P_{cr}$. (b) $\lambda=1.6$ μm, $P=4.5P_{cr}$. (c) $\lambda=1.6$ μm, $P=17.5P_{cr}$, respectively.

*Email address: michaeljs_liu@mail.siom.ac.cn

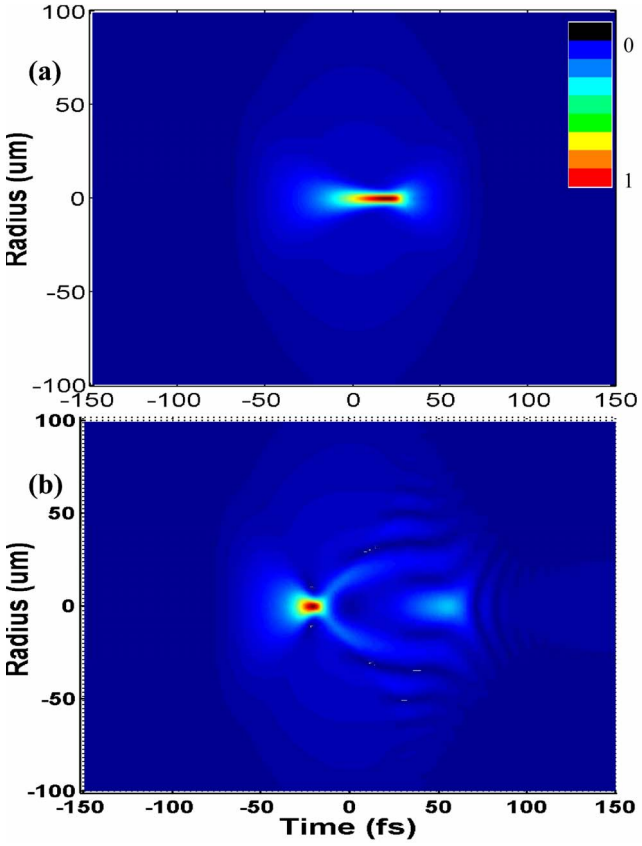

FIG. 2. (Color online) (a), (b) Electric fields $E(r,t)$ in time and space domain at $z=12$ and 13.6 mm, respectively for 800-nm input pulse at $14P_{cr}$.

$+3.17U_p$ [27], where the ponderomotive energy of electrons in laser field U_p is $\propto\lambda^2$, λ is the wavelength of the laser pulse. However due to the ultra-broadband SC, the normal models used to describe the nonlinear propagation of fs laser pulses in the time domain are not any longer suitable for the case in media with anomalous dispersion.

In this paper, by employing a full-order dispersion model formulated in the frequency domain that allows us to investigate the nonlinear dynamics of infrared femtosecond laser pulses propagating in solid media with anomalous GVD both near and above the point at which the pulse effectively undergoes catastrophic collapse, we simulate and analyze the evolutions of the electric field of the laser beam in the filamentation. It is found that different from the *X*-wave generation in normally dispersive media, a spatiotemporally compressed soliton wave with pulse duration of few-cycle oscillations can be generated with the contrary contributions of anomalous GVD and self-phase-modulation. However, as a result of self-steepening, at the tailing edge of the laser pulse forms a shock wave which generates separate and strong SC peaked at ~670 nm due to asymmetric SPM. It is also the origin of colored CE formed both in time and frequency domain with the contribution of normal GVD at visible light. Our simulation result is in good qualitative agreement with the observed SC generated by focusing femtosecond laser pulses at 1.5 μm in silica glass.

Our model for nonlinear propagation of fs pulses in optical media is based on the model developed by Brabec *et al.* [13]. Assuming the pulse has radial symmetry and propagates along z axis with a wave vector $k(\omega)=\frac{n(\omega)\omega}{c}$, where ω is the optical frequency, and $n(\omega)$ is the linear refractive index of the material, the equation of propagation of electric field can be expressed as

$$\partial_z\hat{E}(r,z,\omega)=\left[\frac{i}{2k(\omega)}\nabla_\perp^2+ik(\omega)\right]\hat{E}(r,z,\omega)+\frac{i\omega^2\hat{P}_{NL}(r,z,\omega)}{2k(\omega)c^2\varepsilon_0}-\frac{\omega\hat{J}_f(r,z,\omega)}{2k(\omega)c^2\varepsilon_0},\quad(1)$$

where ε_0 is the dielectric constant in vacuum. $\hat{P}_{\mathrm{NL}}(r,z,\omega)=2\varepsilon_0 n_b n_2 I(r,z,\omega)\otimes E(r,z,\omega)$ is the nonlinear polarization caused by SPM. n_b and n_2 are linear refractive index and nonlinear coefficient respectively. The polarization $J_f(r,z,\omega)$ caused by free electrons has the following form [18]:

$$\hat{J}_f(r,z,\omega)=\frac{e^2}{m(\nu-i\omega)}n_e(r,z,\omega)\otimes\hat{E}(r,z,\omega)+I_p\beta^{(k)}\hat{I}^{(k-1)}(r,z,\omega)\otimes\hat{E}(r,z,\omega)/k_0,\quad(2)$$

where $k_0=0.5c\varepsilon_0$ and ν is the collision frequency. $\beta^{(k)}$ corresponds to the multiphoton ionization (MPI) coefficient and can be calculated by the Keldysh formula [28]. I_p is the gap potential of the material. The evolution of free electron density can be described as $n_e(r,z,t)=\int_{-\infty}^{t}I_{\mathrm{rate}}(r,z,\tau)d\tau$ and $I_{\mathrm{rate}}(r,z,t)=\beta^{(k)}I^k(r,z,t)+\eta_{\mathrm{cas}}n_e(r,z,t)-\eta_{\mathrm{rec}}n_e^2(r,z,t)$, η_{cas} and η_{rec} represent cascade ionization and electron-ion recombination rate, respectively [17,18]. Numerical solutions of Eq. (1) have been shown to accurately reproduce the propagation of laser pulses with duration down to one optical cycle [13,23]. This model combines the advantages of a tractable extended model valid for few-cycle pulses with a correct description of all effects responsible for pulse shortening. It not only accounts for group velocity dispersion, but also high-order dispersive effects.

We investigate the nonlinear dynamics of fs pulses at 1.6 μm propagating in silica glass by numerical integration of Eq. (1). The gap potential for fused silica is $I_p=9.0$ eV, and the number of photons required for ionization is $k=12$. The MPI rate can be calculated as 7.3×10^{-169} m^{21} W^{-12} s^{-1}. The refractive index $n(\omega)$ of silica glass is expressed as a formula given in Ref. [29]. The input laser beam is assumed as a Gaussian profile with a radius of 87 μm ($1/e^2$) and duration of 50 fs [full width at half maximum (FWHM)]. The critical power takes the value [18] $P_{\mathrm{cr}}=\frac{\sqrt{3}\lambda_0^2}{4\pi n_b n_2}=11.1$ MW at $\lambda_0=1.6$ μm for a nonlinear coefficient $n_2=2.2\times10^{-16}$ cm^2/W.

Figures 1(b) and 1(c) show the evolution of peak intensities and beam diameters, respectively, along the propagation axis z for 1.6-μm pulses at different input powers. When the input power increases from $4.5P_{\mathrm{cr}}$ to $17.5P_{\mathrm{cr}}$, the filament is elongated from 2 to 8 mm. As a comparison and shown in Fig. 1(a), we simulated propagation of 800-nm pulse in fused silica at $14P_{\mathrm{cr}}$ ($P_{\mathrm{cr}}=1.9$ MW for 800 nm). The filament for 800-nm pulse is much shorter than that for 1.6 μm pulses.

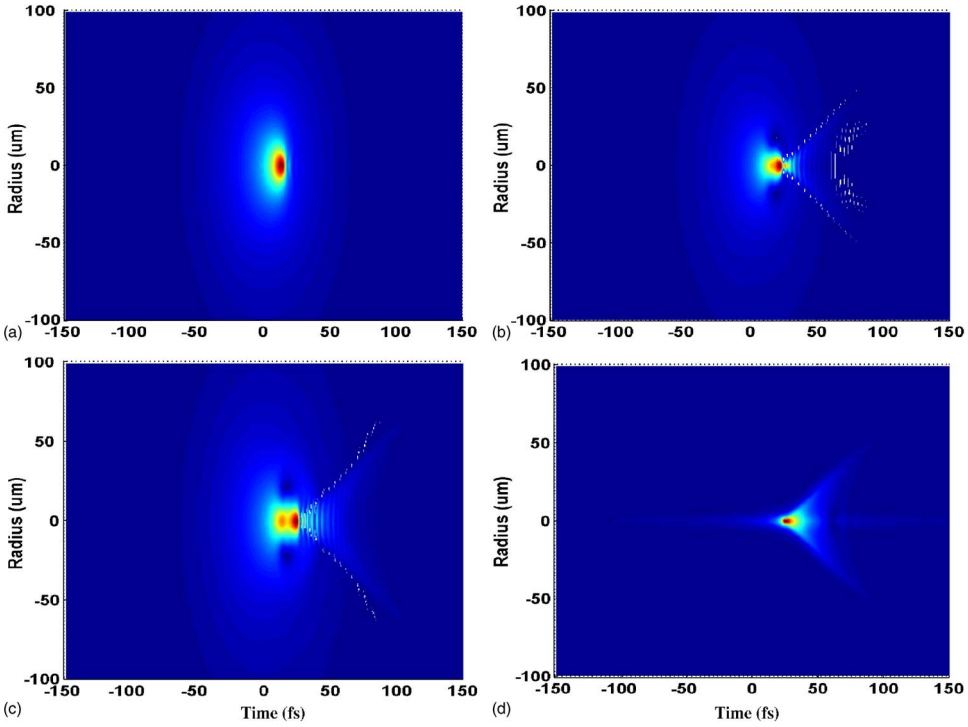

FIG. 3. (Color online) (a)–(c) Electric fields $E(r,t)$ in time and space domain at $z=9.5$, 10.5, and 11.1 mm, respectively, for 1.6 -μm input pulse at $4.5P_{cr}$. (d) Electric field $E(r,t)$ at $z=10.5$ mm corresponding to (b), where infrared component of the spectrum of the electric filed ($\lambda > 800$ nm) is cut out.

This phenomenon has been observed and simulated by Moll *et al.* [24,25]. Although the input power for the 800-nm pulse is much higher than the 1.6-μm pulse in Fig. 1(b), the collapse self-focusing occurs later for the 800-nm pulse. The cause for this is that for the 800-nm pulse normal GVD leads to a broadening of the laser pulse in the beginning of propagation, however, for the 1.6-μm pulse, with the contrary contributions of anomalous GVD and SPM, the laser pulse can experience self-compression both in time and space domain very soon.

In Figs. 2(a) and 2(b) we show the electric field $E(r,t)$ at $z=12$ and 13.6 mm, respectively for the 800-nm input pulse at $14P_{cr}$. It can be seen that an X-shaped electric field is generated at $z=12$ mm before the laser intensity is clamped. However, after further propagation, the on-axis laser pulse splits at $z=13.6$ mm and at the tailing edge forms a conical wave which corresponds to CE. The electric fields $E(r,t)$ at $z=9.5$, 10.5, and 11.1 mm, respectively, for the 1.6-μm input pulse at $4.5P_{cr}$ have been calculated as shown in Figs. 3(a)–3(c). Different from the X-wave generation, a few-cycle spatiotemporal soliton wave is generated as shown in Fig. 3(a). In Fig. 4(a) we show the evolution of laser pulse on axis at $z=8.9$, 9.5, and 9.9 mm, respectively. It is shown that at $z=9.5$ mm generates a few-cycle laser pulse with a duration of 6 fs. However, at the tailing edge of the laser pulse forms a shock wave which has a very steep back edge and can generate strong blue-shifted SC due to asymmetric SPM. The SC generated at $z=10.5$ mm as well as the spectrum of the input pulse are shown in Fig. 4(b). In addition to redshift and broadening of the laser spectra, a separate and blue-shifted SC peaked at 670 nm is generated. It is in qualitative agreement with the observed SC generated by focusing fs pulses at 1.5 μm in silica glass [26].

There are several characteristics about this separate and blueshifted SC. First, it is generated after an shock wave which has a very steep back edge is formed. Due to SPM and plasma, at the back edge the refractive index $n(t)=n_b+n_2I(t)-n_e(t)/2n_c$ (n_c is the critical density of the plasma) decreases as the instant time t increases. The electric wave at later t propagates at a faster speed and will catch up with the electric wave at earlier t, and therefore the back edge steepens and forms a shock wave. Second, the blueshifted SC

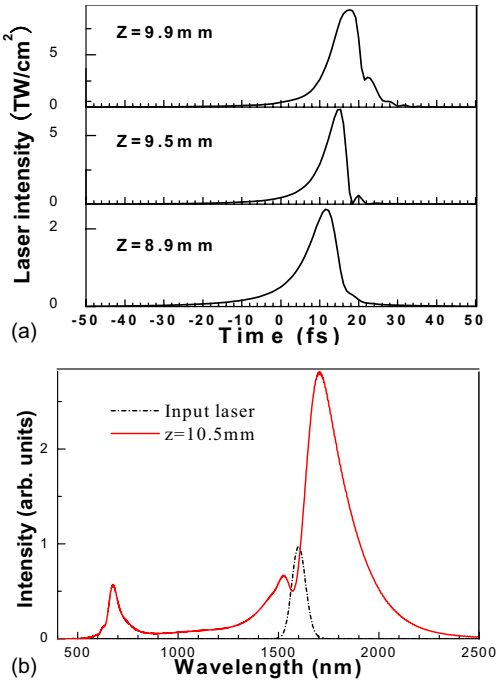

FIG. 4. (Color online) (a) Evolution of laser pulse on axis at $z=8.9$, 9.5, and 9.9 mm for 1.6-μm input pulse at $4.5P_{cr}$, respectively. (b) SC (solid line) generated at $z=10.5$ mm as well as the spectrum (dashed line) of the input pulse.

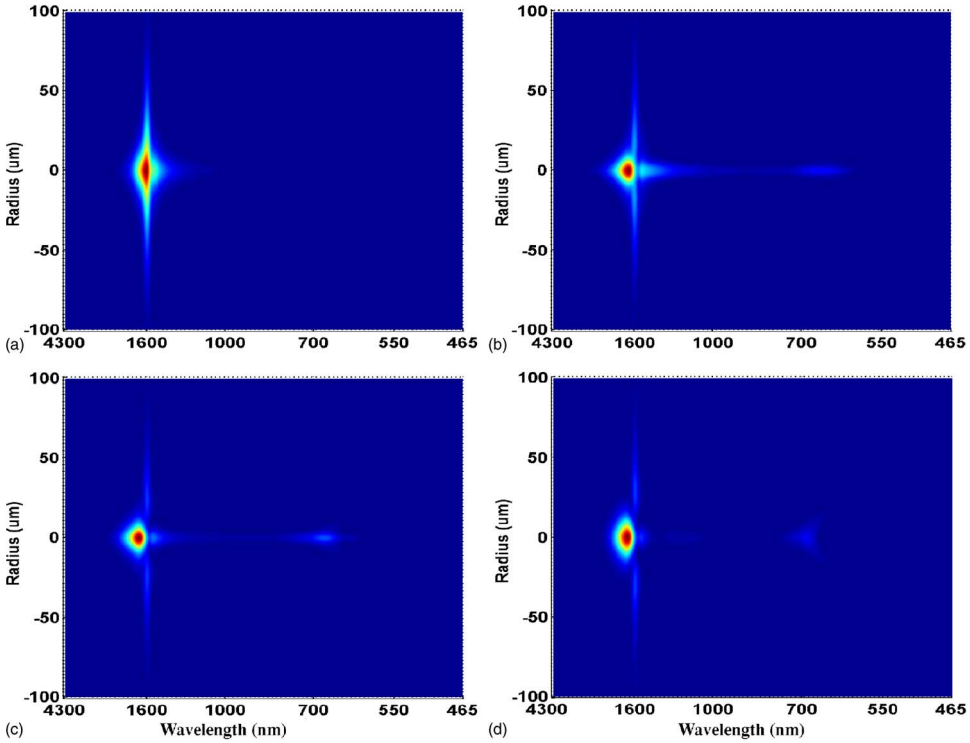

FIG. 5. (Color online) (a)–(d) Spectral intensity distributions $I(r,\lambda)$ in frequency and space domain at $z=9.5$, 10, 10.5, and 11.1 mm, respectively, for 1.6-μm input pulse at $4.5P_{cr}$.

peaked at 670 nm is generated at the back edge of the shock wave due to asymmetric SPM and MPI. In fact, due to SPM and plasma, the process of self-steepening at the back edge of the laser pulse can continue until a vertical edge forms. However, this process of self-steepening can be stopped by the normal GVD of the material at the blueshifted SC because the electric wave at visible light propagates at a slower speed and lags behind to produce frequency chirp. Third, the blueshifted SC peaked at 670 nm propagates in the form of CE in the frequency domain and conical wave in the time domain at the tailing edge of the laser pulse. As shown in Figs. 3(b) and 3(c), the electric fields $E(r,t)$ at $z=10.5$ and 11.1 mm possess a conical wave at the tailing edge of the laser pulse. If infrared component of the spectrum of the electric filed ($\lambda>800$ nm) is cut out, the electric field at $z=10.5$ mm($\lambda<800$ nm) can be calculated as shown in Fig. 3(d). It can be clearly seen that a conical wave which only includes the blueshifted SC is formed at the back edge of the shock wave. After further propagation, for example, at $z=11.1$ mm, the on-axis laser pulse splits as shown in Fig. 3(c). However, the time span between the two split peaks is much smaller compared to the case in normally dispersive media. The corresponding spectral intensity distributions $I(r,\lambda)$ at $z=9.5$, 10, 10.5, and 11.1 mm are calculated and shown in Figs. 5(a)–5(d), respectively. As the laser pulse propagates in the filament, the laser spectrum broadens and covers a wide range from 0.4 to 3 μm. Especially at visible light, the blue-shifted SC becomes stronger and stronger and forms a peak at 670 nm. The spectral distribution $I(r,\lambda)$ at visible light has also a conical form. It indicates that the blue light spreads outward at a larger angle compared to the red light. However for the generated SC from 0.8 nm to 3 μm, no obvious conical wave is formed.

The conical wave and CE generated at the back edge of the laser pulse can be qualitatively explained by GVD, SPM, and MPI. In principle, the nonlinear propagation of fs pulses is guided by the refractive index $n(r,t)=n_b(r,\omega)+n_2I(r,t)-n_e(r,t)/2n_c$. Due to frequency chirp induced by normal GVD of the material and SPM, the linear refractive index $n_b(r,\omega)$ is implicitly time dependent. In space SPM leads to self-focusing of the laser pulse because it produces a positive lens for a Gaussian beam. In frequency domain, SPM produces redshifted spectrum at the leading edge and blueshifted spectrum at the back edge, and at the same time it produces positive GVD. In the case of normal GVD, the redshifted spectrum which propagates at a fast speed and blueshifted spectrum which propagates at a slow speed locate on the opposite sides of the laser pulse and experience very weak self-focusing or even diverging process due to the

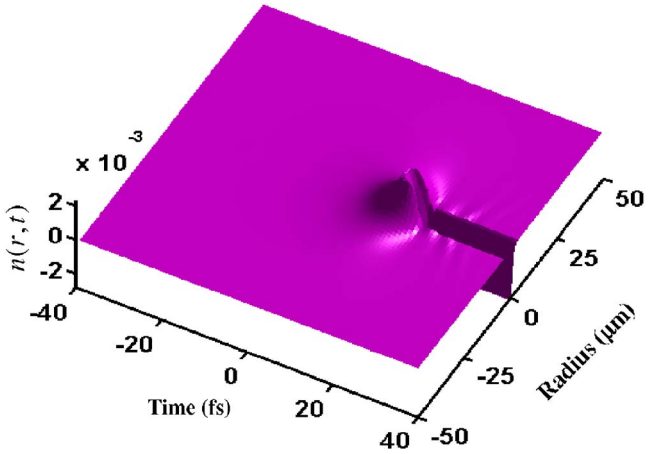

FIG. 6. (Color online) Nonlinear refractive index distribution $n(r,t)$ induced by SPM and free electrons corresponding to Fig. 3(b).

low laser intensities there. This is phase mismatching between the fundamental laser spectrum and generated SC [17,18]. The fundamental laser beam which locates at the central peak of the laser pulse experiences strong self-focusing due to its high intensity and get a minimum beam size at first. That is the cause of *X*-wave generation in normally dispersive media. However, in the case for anomalous dispersion, although SPM produces a redshifted spectrum at the leading edge and a blueshifted spectrum at the back edge of the laser pulse, the redshifted spectrum propagates at a slow speed and the blueshifted spectrum propagates at a fast speed. Therefore the generated redshifted and blueshifted SC on the opposite sides of the laser pulse propagate to the peak and replenish the off-axis zone at the central peak where the strongest self-focusing occurs. That is why a spatiotemporal soliton wave can be formed as shown in Fig. 3(a). However, after a very steep shock wave forms at the back edge of the laser pulse, strong blueshifted SC which has a peak at 670 nm and locates in the regime of normal GVD can be generated due to asymmetric SPM and MPI. This newly generated blueshifted SC propagates at a slow speed and lags behind to produce frequency chirp. In Fig. 6 we show the nonlinear refractive index distribution $n(r,t)$ induced by SPM and free electrons at $z=10.5$ mm. At the back edge of the shock wave forms a negative-lens channel, which will lead to outward spreading of the blueshifted SC at visible light. The blue light spreads outward at a larger angle than the red light because the blue light lags behind and experiences a stronger negative lens. After leaving the negative-lens channel, the blue light propagates at an even slower speed due to normal GVD and thus forms a conical wave.

In conclusion, we investigate the nonlinear dynamics of infrared femtosecond laser pulses propagating in solid media with anomalous GVD by using a full-order dispersion model formulated in frequency domain. Different from the *X*-wave generation in normally dispersive media, spatiotemporally compressed soliton wave with pulse duration of few-cycle oscillations can be generated with the contrary contributions of anomalous GVD and SPM. Compared to normal GVD, anomalous GVD can promote a long self-guiding of the laser beam. In our simulation an optical shock wave formed at the back edge of the laser pulse gives rise to a blueshifted SC which has a peak at 670 nm. It is in good qualitative agreement with the observed SC generated by focusing femtosecond laser pulses at 1.5 μm in silica glass [26]. Because anomalous GVD can compensate the positive GVD caused by SPM, filamentation of infrared pulses in materials with anomalous dispersion favors the generation of ultrabroadband SC from 400–3000 nm and few-cycle laser pulses. It can find applications in laser spectroscopy and pulse-shortening techniques. Our numerical simulations were performed on the Shanghai Supercomputer Center.

[1] P. B. Corkum, C. Rolland, and T. Srinivasan-Rao, Phys. Rev. Lett. **57**, 2268 (1986).
[2] A. Brodeur and S. L. Chin, J. Opt. Soc. Am. B **16**, 637 (1999).
[3] V. P. Kandidov, O. G. Kosareva, I. S. Golubtsov, W. Liu, A. Becker, N. Akozbek, C. M. Bowden, and S. L. Chin, Appl. Phys. B: Lasers Opt. **77**, 149 (2003).
[4] S. Henz and J. Herrmann, Phys. Rev. A **59**, 2528 (1999).
[5] L. Bergé and A. Couairon, Phys. Rev. Lett. **86**, 1003 (2001).
[6] C. P. Hauri, W. Kornelis, F. W. Helbing, A. Heinrich, A. Couairon, A. Mysyrowicz, J. Biegert, and U. Keller, Appl. Phys. B: Lasers Opt. **79**, 673 (2004).
[7] Hélène Ward and Luc Bergé, Phys. Rev. Lett. **90**, 053901 (2003).
[8] J. Kasparian, M. Rodriguez, G. Méjean, J. Yu, E. Salmon, H. Wille, R. Bourayou, S. Frey, Y.-B. André, A. Mysyrowicz, R. Sauerbrey, J. P. Wolf, and L. Wöste, Science **301**, 61 (2003).
[9] G. Y. Yang and Y. R. Shen, Opt. Lett. **9**, 510 (1984).
[10] A. A. Zozulya, S. A. Diddams, A. G. Van Engen, and T. S. Clement, Phys. Rev. Lett. **82**, 1430 (1999).
[11] C. Conti, S. Trillo, P. Di Trapani, G. Valiulis, A. Piskarskas, O. Jedrkiewicz, and J. Trull, Phys. Rev. Lett. **90**, 170406 (2003).
[12] A. L. Gaeta, Phys. Rev. Lett. **84**, 3582 (2000).
[13] T. Brabec and F. Krausz, Rev. Mod. Phys. **72**, 545 (2000).
[14] G. Méchain, A. Couairon, M. Franco, B. Prade, and A. Mysyrowicz, Phys. Rev. Lett. **93**, 035003 (2004).
[15] I. S. Golubtsov, V. P. Kandidov, and O. G. Kosareva, Atmos. Oceanic Opt. **14**, 303 (2001).
[16] A. Couairon, E. Gaižauskas, D. Faccio, A. Dubietis, and P. Di Trapani, Phys. Rev. E **73**, 016608 (2006).
[17] M. Kolesik, E. M. Wright, and J. V. Moloney, Phys. Rev. Lett. **92**, 253901 (2004).
[18] J. Liu, H. Schroeder, S. L. Chin, W. Yu, R. Li, and Z. Xu, Phys. Rev. A **72**, 053817 (2005).
[19] C. Conti, Phys. Rev. E **68**, 016606 (2003).
[20] E. T. J. Nibbering, P. F. Curley, G. Grillon, B. S. Prade, M. A. Franco, F. Salin, A. Mysyrowicz, Opt. Lett. **21**, 62 (1996).
[21] O. G. Kosareva, V. P. Kandidov, A. Brodeur, C. Y. Chien, S. L. Chin, Opt. Lett. **22**, 1332 (1997).
[22] Q. Xing, K. M. Yoo, and R. R. Alfano, Appl. Opt. **32**, 2087 (1993).
[23] A. Couairon, J. Biegert, C. P. Hauri, W. Kornelis, F. W. Helbing, U. Keller, A. Mysyrowicz, J. Mod. Opt. **53**, 75 (2006).
[24] K. D. Moll and A. L. Gaeta, Opt. Lett. **29**, 995 (2004).
[25] L. Bergé and S. Skupin, Phys. Rev. E **71**, 065601(R) (2005).
[26] A. Saliminia, S. L. Chin, and R. Vallée, Opt. Express **13**, 5731 (2005).
[27] P. B. Corkum, Phys. Rev. Lett. **71**, 1994 (1993).
[28] L. V. Keldysh, Sov. Phys. JETP **20**, 1307 (1965).
[29] G. P. Agrawal, *Fiber-Optic Communication Systems*, 2nd ed. (Wiley-Interscience, New York, 1997).